REVIEW OF SCIENTIFIC INSTRUMENTS **79**, 10E502 (2008)

First measurements of the absolute neutron spectrum using the magnetic recoil spectrometer at OMEGA (invited)[a]

J. A. Frenje,[1] D. T. Casey,[1] C. K. Li,[1] J. R. Rygg,[1,b] F. H. Séguin,[1] R. D. Petrasso,[1,c]
V. Yu Glebov,[2] D. D. Meyerhofer,[2] T. C. Sangster,[2] S. Hatchett,[3] S. Haan,[3] C. Cerjan,[3]
O. Landen,[3] M. Moran,[3] P. Song,[3] D. C. Wilson,[4] and R. J. Leeper[5]
[1]*Plasma Science and Fusion Center, Massachusetts Institute of Technology, Cambridge, Massachusetts 02139, USA*
[2]*Laboratory for Laser Energetics, University of Rochester, Rochester, New York 14623, USA*
[3]*Lawrence Livermore National Laboratory, Livermore, California 94550, USA*
[4]*Los Alamos National Laboratory, New Mexico 87545, USA*
[5]*Sandia National Laboratory, New Mexico 87123, USA*

(Presented 12 May 2008; received 10 May 2008; accepted 13 June 2008;
published online 31 October 2008)

A neutron spectrometer, called a magnetic recoil spectrometer (MRS), has been built and implemented at the OMEGA laser facility [T. R. Boehly *et al.*, Opt. Commun. **133**, 495 (1997)] for absolute measurements of the neutron spectrum in the range of 6–30 MeV, from which fuel areal density (ρR), ion temperature (T_i), and yield (Y_n) can be determined. The results from the first MRS measurements of the absolute neutron spectrum are presented. In addition, measuring ρR at the National Ignition Facility (NIF) [G. H. Miller *et al.*, Nucl. Fusion **44**, S228 (2004)] will be essential for assessing implosion performance during all stages of development from surrogate implosions to cryogenic fizzles to ignited implosions. To accomplish this, we are also developing an MRS for the NIF. As much of the research and development and instrument optimization of the MRS at OMEGA are directly applicable to the MRS at the NIF, a description of the design and characterization of the MRS on the NIF is discussed as well. © *2008 American Institute of Physics.*

[DOI: 10.1063/1.2956837]

I. INTRODUCTION

Proper assembly of capsule mass, as manifested through evolution of fuel areal density (ρR),[1–3] is fundamentally important for achieving hot-spot ignition planned at the National Ignition Facility (NIF).[4] Experimental information about ρR and ρR symmetries, as well as T_i and Y_n, is therefore absolutely essential for understanding how assembly occurs and critically evaluating numerical simulations during all stages of development from surrogate implosions to cryogenic fizzles to ignited implosions. To obtain this information, we are currently developing a neutron spectrometer, a magnetic-recoil spectrometer (MRS), whose primary objective is to measure the absolute spectrum in the range of 6–30 MeV, from which ρR, T_i, and Y_n can be directly inferred. Important to the design is that the MRS covers all essential details of the neutron spectrum. A fuel ρR can be inferred from the measured spectrum of the down-scattered neutrons in the range of 6–10 MeV. Measurement of the tertiary spectrum (>20 MeV) allows a second determination of the ρR for high-yield implosions, which can be compared directly to the down-scattered neutron inferred ρR. Having such self-consistency check could prove immensely important for NIF fizzles that are on the threshold to ignite. In addition, absolute yield and a highly resolved 14 MeV primary neutron spectrum can be measured. This allows for measurements of T_i and, possibly more interestingly, nonthermal features, deviations from a single temperature, and the effect of α-particle heating that might give an insight into the nature of failed ignition-capsule implosions that have, for example, substantial cold high-density plasma that surrounds a hot low-density plasma.

A prototype MRS has been built on OMEGA (Ref. 5) to comprehensively test the technique, and provide experience for designing an optimal MRS for the NIF. There are other important reasons for taking this approach. First, ρR of both surrogate and cryogenic DT implosions can be inferred from both the MRS and charged-particle spectrometry (CPS) [with knock-on deuterons (KO-Ds)] for moderate ρR implosions ($\rho R < 200\ \mathrm{mg/cm^2}$);[6–8] this allows for a definitive check of the MRS. Second, as there are no other ways to determine cryogenic $\rho R > 200\ \mathrm{mg/cm^2}$ at OMEGA, the MRS brings the required diagnostic to the OMEGA cryogenic program.

This paper is structured as follows: Sec. II describes the inertial confinement fusion (ICF) neutron spectrum and how it can be used to determine ρR, T_i, multi-T_i, nonthermal features, the effect of α-particle heating, and Y_n. Sections III and IV discuss the design and characterization, respectively, of the MRS at OMEGA and the NIF. Section V presents the

---

[a] Invited paper, published as part of the Proceedings of the 17th Topical Conference on High-Temperature Plasma Diagnostics, Albuquerque, New Mexico, May 2008

[b] Present address: Lawrence Livermore National Laboratory, Livermore, CA 94550.

[c] Visiting Senior Scientist at the Laboratory for Laser Energetics, University of Rochester, Rochester, NY 14623.

0034-6748/2008/79(10)/10E502/6/$23.00

© 2008 American Institute of Physics

Downloaded 12 Jul 2011 to 198.125.177.149. Redistribution subject to AIP license or copyright; see http://rsi.aip.org/about/rights_and_permissions

results from the first measurements of the neutron spectrum using the MRS at OMEGA, while Sec. VI presents MRS measurements of the KO-D spectrum, from which ρR can be directly inferred. Section VII summarizes the paper.

II. THE ICF NEUTRON SPECTRUM

In an ICF implosion, primary neutrons are produced primarily via the reaction

$$\mathrm{D} + \mathrm{T} \rightarrow n(14.1\ \mathrm{MeV}) + \alpha(3.5\ \mathrm{MeV}). \tag{1}$$

The primary DT neutrons carry a wealth of information about the ICF implosion, such as information about T_i, multi-T_i, possible nonthermal features, and Y_n.[9] For a single-temperature plasma, T_i can be determined from the Doppler width (ΔE_D) of the primary neutron spectrum [to the first order, $T_i \approx (\Delta E_D/177)^2$ keV],[9] which is represented accurately by a single-Gaussian distribution. The effect of multi-T_i (caused by, for instance, temperature profiles) and nonthermal features would simply show up as deviations from the single-Gaussian distribution. The nonthermal feature could, for instance, be generated by a strong, localized electrical field, which originates from the pressure gradient inside the implosion,[10] causing strong bulk flows at high velocities on the order of the sound speed.

In a secondary process, a small fraction of the primary neutrons elastically scatter off the fuel ions [primarily deuterons (D) and tritons (T)] as described by

$$n + \mathrm{D} \rightarrow n'(1.6-14.1\ \mathrm{MeV}) + \mathrm{D}'(<12.5\ \mathrm{MeV}), \tag{2}$$

$$n + \mathrm{T} \rightarrow n'(3.5-14.1\ \mathrm{MeV}) + \mathrm{T}'(<10.6\ \mathrm{MeV}). \tag{3}$$

By using a relatively simple model of an implosion, the ρR can be related to the down-scattered neutron yield $(Y_{n'})$ by

$$\rho R \approx \frac{(2\gamma+3)m_p}{(\gamma\sigma_d+\sigma_t)}\frac{Y_{n'}}{Y_n}, \tag{4}$$

where $\gamma = n_d/n_t$, σ_d and σ_t are the effective elastic scattering cross sections for deuterons and tritons, respectively, m_p is the proton mass, $Y_{n'}$ is the measured down-scattered neutron yield in a certain defined energy range, and Y_n is the measured primary neutron yield. As shown by Eq. (4), the fuel ρR is linearly proportional to the yield ratio of down-scattered neutrons (n') and primary neutrons (n).[8]

As scattered high-energy deuterons (D′) or tritons (T′), produced in processes (2) and (3), pass through the fuel, some undergo tertiary reactions and produce tertiary neutrons (n''):

$$\mathrm{D}' + \mathrm{T} \rightarrow \alpha(0.1-18.1\ \mathrm{MeV}) + n''(12.0-30.1\ \mathrm{MeV}), \tag{5}$$

$$\mathrm{T}' + \mathrm{D} \rightarrow \alpha(<19.0\ \mathrm{MeV}) + n''(9.2-28.2\ \mathrm{MeV}). \tag{6}$$

According to LASNEX simulations,[11] the yield of the tertiary neutrons (>20 MeV) is of the order of 10^{-6} relative to the primary neutron yield and proportional to ρR and ρR^2 for high-ρR and low-ρR implosions, respectively.

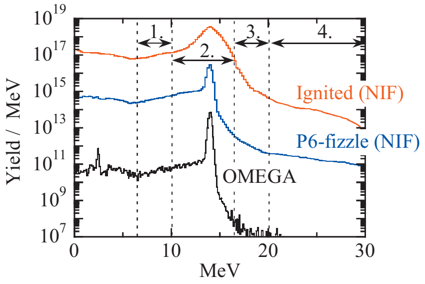

FIG. 1. (Color) Neutron spectra simulated by LASNEX for an OMEGA (black line) and two NIF (blue and red lines) cryogenic DT implosions. For the OMEGA implosion, a down-scattered neutron yield of 1.5×10^{11} (region 1), corresponding to a fuel ρR of 128 mg/cm^2, and primary neutron yield of 2.4×10^{13} were simulated. For the NIF, a neutron spectrum was simulated for an ignited (red line) and a P_6-fizzle (blue line) implosion. For the ignition case, a down-scattered yield of 3.6×10^{17} and primary yield of 7.4 $\times10^{18}$ were simulated. A significant tertiary component (region 4) of 1.5 $\times10^{15}$ was simulated as well. For the "P_6 fizzle," a down-scattered yield of 1.5×10^{15}, primary yield of 2.1×10^{16}, and tertiary yield of 2.0×10^{12} were simulated. A ρR of ~2 g/cm^2 was simulated for both NIF implosions. The nonthermal, secondary-neutron component, originating from the α-particle interaction with the fuel ions, dominates at energies in the range of 16–20 MeV (region 3). Secondary-neutron yields of 1.5×10^{8}, 6.8×10^{12}, and 9.0×10^{16} were simulated for the OMEGA, NIF-P_6-fizzle, and NIF-ignition implosions, respectively.

When the α particles, produced in reaction (1), interact with the plasma, they lose energy mainly through small angle scattering with electrons. However, there is a finite probability that the α particles ftransfer several MeV to the D or T by large angle Coulomb or nuclear-elastic scattering. These collisions give rise to nonthermal distributions of fuel ions, which can in turn react with the thermal ions, generating a secondary component in the neutron spectrum. Although with much lower intensity than the primary component (~10^{-5} to ~10^{-2} depending on the implosion), the secondary-neutron component dominates at energies in the range of 16–20 MeV. As the intensity of the secondary-neutron component is strongly sensitive to electron temperature (T_e), measurement of this component could, in principle, address T_e in the high-density region, the effect of α-particle heating, and fuel-ablator mix.

A few typical neutron spectra simulated by LASNEX for OMEGA and the NIF are shown in Fig. 1. These spectra are based on all possible reaction processes starting with the DT and DD reactions. A fuel ρR can be inferred from the down-scattered neutrons in region 1. T_i, multi-T_i, Y_n, possible nonthermal features can be determined from the primary peak in region 2. The effect of α-particle interaction with thermal fuel ions can be determined from the secondary neutrons in region 3, and a second ρR for high-yield implosions can be derived from the tertiary neutron spectrum in region 4.

III. DESIGN OF THE MRS AT OMEGA AND THE NIF

The MRS has three main components (see Fig. 2). The first component is a CH (or CD) foil positioned as close as possible to the implosion[12] to produce recoil protons (or deuterons) from incident neutrons. The second component is a focusing magnet, located outside the target chamber in the case of OMEGA and located outside the target-bay area in the case of the NIF,[13] for energy dispersion and focusing of forward-scattered recoil particles onto the focal plane of the spectrometer. The focusing provides a clear mapping between the position at the focal plane and energy of the proton

Downloaded 12 Jul 2011 to 198.125.177.149. Redistribution subject to AIP license or copyright; see http://rsi.aip.org/about/rights_and_permissions

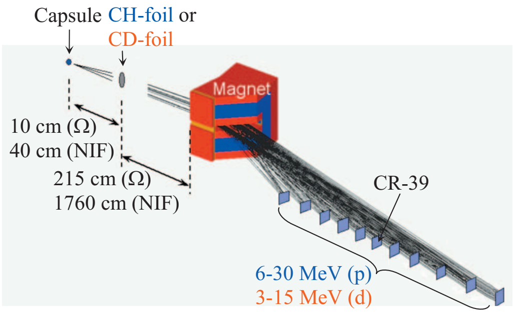

FIG. 2. (Color) A schematic drawing of the MRS, including the foil, magnet, and CR-39 detectors. The foil is positioned as close as possible to the implosion (10 cm in the case of OMEGA and 40 cm in the case of the NIF); the magnet is positioned outside the target chamber in the case of OMEGA (215 cm to the foil) and outside the target-bay wall in the case of the NIF (1760 cm to the foil). Important to the MRS design is that the same magnet design can be used on OMEGA and the NIF. In the case OMEGA, eleven 6×5 cm^2 CR-39 detectors are positioned at the focal plane of the spectrometer for detection of the forward-scattered recoil protons (or deuterons) when using a CH foil (or CD foil). The trajectories shown are for proton energies from 6 to 30 MeV, corresponding to deuteron energies from 3 to 15 MeV. For protons, the dispersion is ~30 keV/mm at 6 MeV and ~70 keV/mm at 25 MeV. These numbers are reduced with a factor of 2 for the deuterons.

(or deuteron), and thus the energy of the neutron that scattered it. The third component is an array of CR-39 detectors, positioned at the focal plane of the spectrometer, which records the position of each recoil particle with a detection efficiency of 100%.[14] By measuring the recoil-particle spectrum, the neutron spectrum is indirectly measured as the MRS response function is well known.

An important characteristic to the MRS design is that the detection efficiency ($\varepsilon_{\mathrm{MRS}}$) for a given response function [energy resolution (ΔE_{MRS})] is maximized. This is achieved by using an aperture in front of the magnet that selects recoil particles scattered in the forward direction at which the *np*- and *nd*-differential elastic scattering cross sections have their maxima in the laboratory system and ΔE_{MRS} has its minimum due to the shortest average path length of the recoil particles in the foil.[15] In this context, it is also important to note that the magnet, which is made of neodymium-iron-boron (NdFeB), is a focusing device with a pole gap of 3 cm, producing a magnetic field up to ~0.9 T and a field gradient of ~60 G/cm. This feature is critical to the MRS design as it allows for the largest possible solid angle to be used, which maximizes $\varepsilon_{\mathrm{MRS}}$ for a defined ΔE_{MRS}. The entrance and exit pole boundaries are also angled relative to the incoming and outgoing particles, as discussed in principle in Ref. 15, for increased focusing properties in both the transverse and dispersive planes, where the former prohibits the recoil particles from hitting the pole boundaries and the latter provides for increased resolving power.

For the MRS to be both practical and useful at OMEGA and the NIF, it has been designed with the highest possible $\varepsilon_{\mathrm{MRS}}$ for a given ΔE_{MRS}, the largest possible dynamic range, and insensitivity to different types of background. Built-in flexibility has also been included in the design to effectively use the MRS for different applications. This is important, as a trade-off between $\varepsilon_{\mathrm{MRS}}$ and ΔE_{MRS} must be applied depending on the application. For instance, for a practical implementation of low-yield applications, such as measurements of down-scattered and secondary neutrons at OMEGA for which yields are orders of magnitude smaller than the primary yield (see Fig. 1), it is necessary to degrade ΔE_{MRS} to substantially increase $\varepsilon_{\mathrm{MRS}}$. For high-yield applications, on the other hand, such as measurements of primary neutron spectrum at OMEGA and the NIF, the MRS can be configured to operate in a high-resolution–low-$\varepsilon_{\mathrm{MRS}}$ mode. Several options are available for configuring the MRS. Either a CH or CD can be selected to produce recoil protons or deuterons (and thus whether the energy range covered for neutrons is 6–30 MeV or 3.4–16.9 MeV). The foil area and thickness can be adjusted to change the $\varepsilon_{\mathrm{MRS}}$ and ΔE_{MRS}. The area of the aperture in front of the magnet can be adjusted as well.

As CR-39 detectors are used in the MRS, the principal sources of background are primary neutrons and neutrons scattered by the chamber wall, diagnostics, and other structures surrounding the MRS. Soft and hard x rays are not an issue, since CR-39 is immune to these types of radiation. Although the CR-39 efficiency for detecting primary neutrons is small[16] ($\varepsilon_{\text{CR-39}} \approx 6 \times 10^{-5}$), reduction in the neutron background is required for successful implementation of the MRS down-scattered neutron measurements. To reduce the neutron background to the required level for down-scattered neutron measurements at OMEGA [a signal-to-background (S/B) ratio of least 10 is required],[17] polyethylene shielding was applied to the MRS as a first step. As the CR-39 detector array is positioned on an off-axis detection plane that is well outside the target chamber, enough space exists to position ~2200 lb of polyethylene shielding in front and around the MRS. A 60 lb stainless steel plug was also placed in between the implosion and the MRS detector array to allow additional attenuation of direct, primary neutrons because of the relatively high inelastic scattering cross sections in iron, chromium, and nickel. Through measurements and neutron-transport simulations using the Monte-Carlo code TART,[18] we have established that the shielding reduces the neutron fluence ~40 times to a fluence of $\sim 2 \times 10^{-8}$ cm^{-2} per produced neutron at the MRS detector array.[19] Figure 3(a) shows the final engineering design of the MRS on OMEGA. In contrast, shielding around the MRS is not required at the NIF as the system is protected by 1.8 m of concrete [see Fig. 3(b)].[17]

For successful implementation of the down-scattered neutron measurements at OMEGA, additional reduction in the neutron background is required. This is accomplished through the use of the coincidence counting technique (CCT), which utilizes the fact that incident signal particles pass straight through the CR-39 if it is thin enough, resulting in coincident front-side and back-side tracks. Real signal tracks can therefore be distinguished easily from neutron-induced tracks, as the latter produce only a track on either the front or back side of the CR-39. When applying the CCT to the MRS data, the S/B ratio can be expressed as[17]

$$\left(\frac{\mathrm{S}}{\mathrm{B}}\right)_{\mathrm{CCT}} \approx \frac{A}{\pi r_c^2}\frac{S}{(S+B)^2}, \tag{7}$$

where A is the signal-detection area, r_c is the correlation radius used when searching for coincident front-side and

Downloaded 12 Jul 2011 to 198.125.177.149. Redistribution subject to AIP license or copyright; see http://rsi.aip.org/about/rights_and_permissions

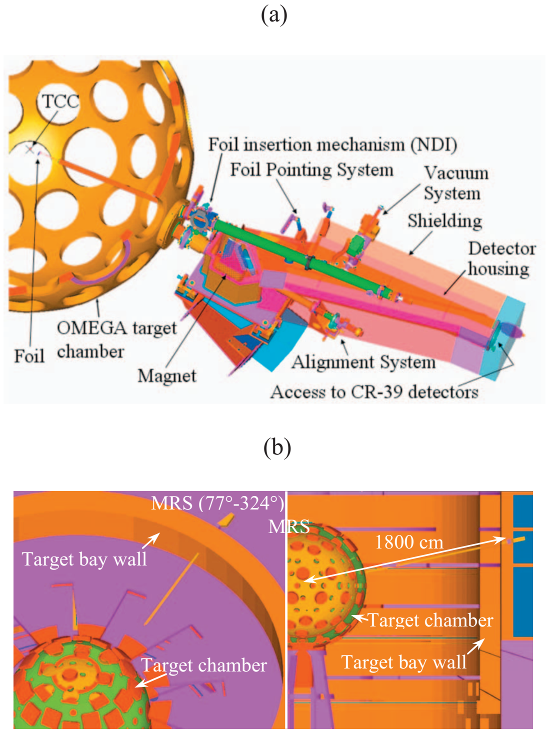

FIG. 3. (Color) (a) Engineering design of the MRS on OMEGA. The foil is inserted by the Nuclear Diagnostics Inserter to 10 cm from target-chamber center (TCC). The MRS magnet, magnet housing, detector housing and shielding are shown in the figure. The total weight of the MRS is ~4100 lb including the ~2200 lb of polyethylene shielding. (b) Conceptual design of the MRS on the NIF. The current plan is to position the MRS outside the target-bay wall (1.8 m of concrete) on the line of sight 77°–324°.

back-side tracks, S is number of signal tracks produced by down-scattered neutrons in the energy range of 6–10 MeV, and B is the total number of background tracks observed in the detection area. For low signal and background track densities, the $(S/B)_{\mathrm{CCT}}$ ratio is typically of the order of 10^2–10^3, a result of the fact that $A/\pi r_c^2$ is a large number. As the signal and background track densities increase, the $(S/B)_{\mathrm{CCT}}$ ratio decreases due to an increasing number of random coincidences. In addition, it should be noted that the CCT does not have to be applied to the down-scattered neutron data obtained at the NIF, as the MRS is behind 1.8 m of concrete [see Fig. 3(b)], which is thick enough to reduce the neutron background to an acceptable level of $\sim 5\times 10^{-12}$ cm^{-2} per produced neutron. S and B in Eq. (7) can be expressed as[17]

$$S \approx 0.03\rho R(\mathrm{g/cm^2})Y_n\varepsilon_{\mathrm{MRS}}, \tag{8}$$

$$B \approx 2\times 10^{-8} A Y_n \varepsilon_{\text{CR-39}}, \quad (\text{OMEGA}), \tag{9}$$

$$B \approx 5\times 10^{-12} A Y_n \varepsilon_{\text{CR-39}} \quad (\text{NIF}). \tag{10}$$

Here, $\varepsilon_{\mathrm{MRS}}$ is discussed in Sec. IV, and A is ~75 and ~25 cm^2 for the down-scattered neutron measurements at OMEGA and the NIF, respectively. For primary neutron measurements, Eq. (8) should be modified to $S \approx Y_n\varepsilon_{\mathrm{MRS}}$.

IV. CHARACTERIZATION OF THE MRS AT OMEGA AND THE NIF

GEANT4 (Ref. 20) and a developed Monte-Carlo code were used to characterize the performance of the different MRS-operating configurations at OMEGA and the NIF. The results from that modeling are shown in Table I for the down-scattered neutron measurements in the energy range of 6–10 MeV. The first and second columns are for the MRS operating in a low-$\varepsilon_{\mathrm{MRS}}$ and high-$\varepsilon_{\mathrm{MRS}}$ mode at OMEGA, respectively. The third and fourth columns are for the MRS operating in a low-$\varepsilon_{\mathrm{MRS}}$ and a high-$\varepsilon_{\mathrm{MRS}}$ mode at the NIF, respectively. The difference between these two configurations at OMEGA and the NIF is due to the different foil characteristics. For primary neutron measurements, $\varepsilon_{\mathrm{MRS}}$ and ΔE_{MRS} numbers, shown in Table I, should be reduced by ~40%. In addition, the high-$\varepsilon_{\mathrm{MRS}}$ mode is applied mainly to down-scattered neutron measurements at OMEGA, while low-$\varepsilon_{\mathrm{MRS}}$ mode is applied normally to high-resolution studies of primary neutron spectrum. High-resolution studies can also be applied to down-scattered neutron measurements when $Y_{n'}$ is high enough.

TABLE I. Detection efficiency ($\varepsilon_{\mathrm{MRS}}$) and energy resolution (ΔE_{MRS}) for two different MRS configurations at OMEGA and the NIF. The first and second columns are for the MRS operating in a low-$\varepsilon_{\mathrm{MRS}}$ and a high-$\varepsilon_{\mathrm{MRS}}$ mode at OMEGA, respectively. The third and fourth columns are for the MRS operating in a low-$\varepsilon_{\mathrm{MRS}}$ and a high-$\varepsilon_{\mathrm{MRS}}$ mode at the NIF, respectively. These numbers are for measurements of down-scattered neutrons when using a CD foil. A factor of 2 thicker CH foil provides about the same $\varepsilon_{\mathrm{MRS}}$ and ΔE_{MRS}. In addition, the $\varepsilon_{\mathrm{MRS}}$ and ΔE_{MRS} numbers should be reduced by ~40% for the primary neutron measurements.

	OMEGA		NIF	
Configuration	1	2	1	2
CD-foil distance (cm)	10	10	40	40
CD-foil thickness (μm)	40	290	40	290
CD-foil area (cm^2)	4.0	13	20	20
Magnet aperture (cm)	22	22	20	20
Magnet aperture distance (cm)	215	215	1760	1760
ΔE_{MRS} (FWHM) (MeV)	0.5	2.0	0.4	1.8
$\varepsilon_{\mathrm{MRS}}$ ($\times 10^{-11}$)	35	820	0.15	1.1

The signal-to-noise (S/N) and signal-to-background (S/B) ratios for the down-scattered neutron measurements at OMEGA and the NIF can now be determined from Eqs. (7)–(10) and Table I. The results are summarized in Table II. for a warm DT filled CH implosion at OMEGA and the cryogenic DT implosions discussed in Sec. II. As illustrated by the S/B numbers shown in Table II, the S/N ratios are dictated mainly by the signal. Both in terms of S/N and S/B, it is clear that the MRS will accurately diagnose the ρR in these implosions using down-scattered neutrons.

As the CR-39 detects the recoil particles with 100% efficiency and B is small in comparison, the MRS dynamic range is determined mainly by signal statistics and signal saturation. About $\sim 10^2$ signal counts are required to infer a fuel ρR from the down-scattered neutron spectrum, and $\sim 10^7$ signal counts over the signal-detection area are required for the CR-39 to saturate.[14] This results in a single shot dynamic range of $\sim 10^5$. An additional factor of 10 is achieved due to the flexibility built into the design.

Downloaded 12 Jul 2011 to 198.125.177.149. Redistribution subject to AIP license or copyright; see http://rsi.aip.org/about/rights_and_permissions

TABLE II. Signal-to-noise (S/N) and signal-to-background (S/B) ratios for the different MRS configurations, shown in Table I, planned to be used for the down-scattered neutron measurements (6–10 MeV) at OMEGA and the NIF. The CCT [Eq. (7)] has only been applied to the OMEGA data when using a correlation radius of 50 μm. As Y_n is at least two orders of magnitude higher than $Y_{n'}$, the S/B and S/N ratios for the primary neutron measurements is at least factors of 100 and 10 higher, respectively.

Facility	Implosion	ρR (g/cm^2)	Y_n	S/N 1	S/N 2	S/B 1	S/B 2
OMEGA	Warm	0.07	10^{13}	3	13	15	230
	Cryo	0.13	2×10^{13}	5	25	14	154
NIF	P_6 fizzle	2.0	2×10^{16}	42	115	12	88
	Ignited	1.9	7×10^{18}	245	2095	11	84

V. MRS ACTIVATION AND CALIBRATION EXPERIMENTS

For the MRS activation and calibration experiments, a series of DT filled CH capsules with a nominal diameter of 850 μm, a fill pressure of 15 atm, and a shell thickness of 15 μm was imploded with a 1 ns square laser pulse shape delivering ~23 kJ of UV energy on capsule. All laser beams on OMEGA were smoothed with SG3 distributed phase plates,[21] 1 THz, two-dimensional smoothing by spectral dispersion,[22] and polarization smoothing using birefringement wedges.[23] The beam-to-beam energy imbalance was typically 3% rms for these implosions.

A primary neutron yield from $\sim10^{13}$ to $\sim3\times10^{13}$ and a T_i in the range of 5–6 keV were produced in these implosions. An accurate yield and energy calibration of the MRS could therefore be obtained as these yields were high enough to allow the MRS to operate in a high-resolution mode (configuration 1 shown in Table I). Fourteen implosions were used for these experiments. For each shot, a tantalum (Ta) filter, with a certain thickness, was positioned just behind the CH (or CD) foil to range down the energy of the recoil protons (or deuterons) [see Fig. 4(a)]. This allowed for an accurate energy calibration of the MRS in the range of 6–25 MeV (proton equivalent energy). The energies above 14 MeV are accessible using recoil deuterons from a CD foil. Figure 4(b) shows a subset of three measured spectra that are compared to the GEANT4 modeling of the MRS. A Ta filter with thicknesses of 80 and 140 μm was positioned just behind the CH foil to range down the recoil-proton spectrum to 12 and 10 MeV, respectively. As is illustrated in Fig. 4(b), excellent agreement exists between measured and simulated Y_n, average energy, and spectral shape, indicating that the GEANT4 modeling of the MRS is accurate.

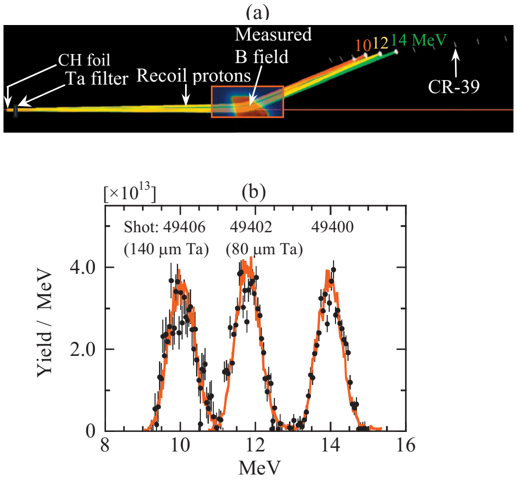

FIG. 4. (Color) (a) GEANT4 modeling of the MRS activation and calibration experiments using primary neutrons from three DT filled CH-capsule implosions. In the first measurement, 14 MeV recoil protons were momentum analyzed and detected. In the last two measurements, a Ta filter with thicknesses 80 of and 140 μm was positioned just behind the CH foil to range down the recoil-proton spectrum to 12 and 10 MeV, respectively. (b) Measured and simulated recoil-proton spectra. The measured spectra agree with the GEANT4 modeling in terms of yield, average energy, and spectral shape, which indicates that the predicted performance of the MRS is accurate. Y_n of $(3.0\pm0.3)\times10^{13}$, $(3.3\pm0.2)\times10^{13}$, and $(3.0\pm0.2)\times10^{13}$ were determined for shots 49406, 49402, and 49400, respectively. It is important to note that these calibration measurements were performed without the shielding installed.

The whole set of MRS data obtained during these experiments is illustrated in Fig. 5. The measured and simulated average energies as a function of position along the focal plane are shown in Fig. 5(a), and the MRS determined yields contrasted to the neutron time of flight (nTOF) yields are shown in Fig. 5(b). Both sets of data indicate clearly that the MRS performance is well understood both in terms of energy and ε_{MRS} for practically the whole energy-band width of the MRS.

VI. ρR MEASUREMENTS USING THE MRS

MRS measurements of particles produced in secondary processes [Eqs. (2) and (3)] have just begun. In particular, spectra of KO-D for cryogenic DT implosions have been

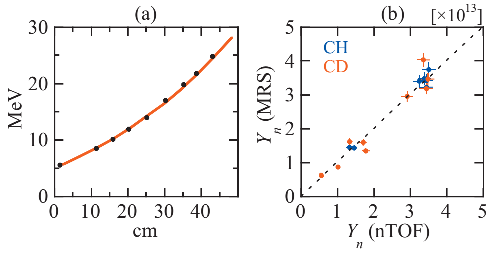

FIG. 5. (Color) (a) Measured and simulated average energies of the recoil-proton (or recoil-deuteron) spectrum, obtained from nine shots, vs position along the focal plane. (b) Y_n measured by MRS and nTOF for 14 shots. Both sets of data indicate clearly that the MRS performance is well understood for practically the whole energy band width.

Downloaded 12 Jul 2011 to 198.125.177.149. Redistribution subject to AIP license or copyright; see http://rsi.aip.org/about/rights_and_permissions

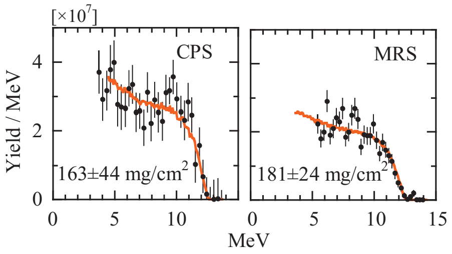

FIG. 6. (Color) CPS and MRS measured KO-D spectra for the low-yield, low-adiabat cryogenic DT implosion 50515. Also shown are simulated fits (red lines) to the measured spectra. From the fits, ρR of 163 ± 44, and 181 ± 24 were determined from the CPS and MRS data, respectively.

obtained when the MRS was operated in a charged-particle mode (no foil close to the implosion). An example of the resulting data from those measurements is shown in Fig. 6 and compared to data taken by a standard CPS.[14] Through Monte-Carlo modeling of a cryogenic DT implosion, it has been established that the fuel ρR can be determined accurately from the shape of the KO-D spectrum.[24]

VII. SUMMARY

A neutron spectrometer, called an MRS, has been built and implemented at the OMEGA laser facility for absolute measurements of the neutron spectrum in the range of 6–30 MeV, from which fuel areal density (ρR), ion temperature (T_i), and yield (Y_n) can be determined. The results from the MRS activation and calibration experiments, using primary neutrons, indicate that the MRS performs as predicted. With the MRS shielding installed, particles from secondary reactions have now been measured as well. From spectral measurement of KO-Ds, a fuel ρR of a cryogenic DT implosion has been inferred. These measurements indicate that the MRS concept will work for the down-scattered neutron measurements at OMEGA and, in particular, at the NIF as yields and ρRs will be significantly higher. At the NIF, measurements of the secondary and tertiary components in the neutron spectrum might provide additional insights about the nature of failed ignition-capsule implosions.

ACKNOWLEDGMENTS

The work described here was supported in part by the U.S. DOE (Grant No. DE-FG03-03SF22691), LLE (No. 412160–001G), LLNL (No. B504974), and GA under DOE (DE-AC52-06NA27279).

[1] S. W. Haan, S. Pollaine, J. D. Lindl, L. J. Suter, R. L. Berger, L. V. Powers, W. E. Alley, P. A. Amendt, J. A. Futterman, W. K. Leverdahl *et al.*, Phys. Plasmas **2**, 2480 (1995).

[2] J. D. Lindl, R. L. Mccrory, E. M. Campbell *et al.*, Phys. Today **45**(9), 32 (1992).

[3] M. D. Rosen, Phys. Plasmas **3**, 1803 (1996).

[4] G. H. Miller, E. I. Moses, and C. R. Wuest, Nucl. Fusion **44**, S228 (2004).

[5] T. R. Boehly, D. L. Brown, R. S. Craxton, R. L. Keck, J. P. Knauer, J. H. Kelly, T. J. Kessler, S. A. Kumpan, S. J. Bucks, S. A. Letzring *et al.*, Opt. Commun. **133**, 495 (1997).

[6] S. Skupsky and S. Kacenjar, J. Appl. Phys. **52**, 2608 (1981).

[7] S. Kacenjar, S. Skupsky, A. Entenberg, L. Goldman, and M. Richardson, Phys. Rev. Lett. **49**, 463 (1982).

[8] C. K. Li, F. H. Séguin, D. G. Hicks, J. A. Frenje, K. M. Green, S. Kurebayashi, R. D. Petrasso, D. D. Meyerhofer, J. M. Soures, V. Yu. Glebov *et al.*, Phys. Plasmas **8**, 4902 (2001).

[9] H. Brysk, Plasma Phys. **15**, 611 (1973).

[10] C. K. Li, F. H. Séguin, J. R. Rygg, J. A. Frenje, M. Manuel, R. D. Petrasso, R. Betti, J. Delettrez, J. P. Knauer, F. Marshall *et al.*, Phys. Rev. Lett. **100**, 225001 (2008).

[11] G. Zimmerman and W. Kruer, Comments Plasma Phys. Controlled Fusion **11**, 51 (1975).

[12] The foil needs to be positioned as close as possible to the implosion for a couple of reasons as discussed in Ref. 15. First, the detection efficiency for a defined energy resolution is maximized. Secondly, the number of incoming neutrons, at the foil, that have scattered off the target chamber and internal structures is negligible in comparison to the number of down-scattered neutrons coming from the implosion.

[13] The magnet is positioned well outside the target chamber in the case of OMEGA and outside the target-bay wall in the case of the NIF to allow for significant amount of shielding to be placed in front and around the MRS.

[14] F. H. Séguin, J. A. Frenje, C. K. Li, D. G. Hicks, S. Kurebayashi, J. R. Rygg, B.-E. Schwartz, R. D. Petrasso, S. Roberts, J. M. Soures *et al.*, Rev. Sci. Instrum. **74**, 975 (2003).

[15] J. A. Frenje, K. M. Green, D. G. Hicks, C. K. Li, F. H. Séguin, R. D. Petrasso, T. C. Sangster, T. W. Phillips, V. Yu. Glebov, D. D. Meyerhofer *et al.*, Rev. Sci. Instrum. **72**, 854 (2001).

[16] J. A. Frenje, C. K. Li, F. H. Séguin, D. G. Hicks, S. Kurebayashi, R. D. Petrasso, S. Roberts, V. Yu. Glebov, D. D. Meyerhofer, T. C. Sangster *et al.*, Rev. Sci. Instrum. **73**, 2597 (2002).

[17] D. T. Casey, J. A. Frenje, S. C. McDuffee, C. K. Li, J. R. Rygg, F. H. Séguin, R. D. Petrasso, V. Yu. Glebov, D. D. Meyerhofer, S. Roberts, and T. C. Sangste, Bull. Am. Phys. Soc. **52**, 208 (2007).

[18] D. E. Collen, "TART2002, TART: Monte carlo radiation transport in industrial applications," LLNL Report No. UCRL-JC-148180, 2002.

[19] D. T. Casey, J. A. Frenje, F. H. Séguin. J. R. Rygg, C. K. Li, S. C. McDuffee, M. Manuel, R. D. Petrasso, V. Yu. Glebov, D. D. Meyerhofer, and T. C. Sangste, "Minimizing neutron background for the Magnetic recoil Spectrometer at OMEGA," Rev. Sci. Instrum. (submitted).

[20] S. Agostinelli, J. Allison, K. Amako, J. Apostolakis, H. Araujo, P. Arce, M. Asai, D. Axen, S. Banerjee, G. Barrand *et al.*, Nucl. Instrum. Methods Phys. Res. A **311**, 595 (1992).

[21] Y. Lin, T. J. Kessler, and G. N. Lawrence, Opt. Lett. **20**, 764 (1995).

[22] S. Skupsky, R. W. Short, T. Kessler, R. S. Craxton, S. Letzring, and J. M. Soures, J. Appl. Phys. **66**, 3456 (1989).

[23] T. R. Boehly, V. A. Smalyuk, D. D. Meyerhofer, J. P. Knauer, D. K. Bradley, R. S. Craxton, M. J. Guardalben, S. Skupsky, and T. J. Kessler, J. Appl. Phys. **85**, 3444 (1999).

[24] J. A. Frenje, C. K. Li, J. R. Rygg, F. H. Séguin, D. T. Casey, R. D. Petrasso, J. Delettrez, V. Yu. Glebov, T. C. Sangster, O. Landen, and S. Hatchett, "Diagnosing fuel areal density (ρR) of cryogenic DT implosions using charged-particle spectrometry at OMEGA," Phys. Plasmas (to be published).

Downloaded 12 Jul 2011 to 198.125.177.149. Redistribution subject to AIP license or copyright; see http://rsi.aip.org/about/rights_and_permissions